Journal of Atomic and Molecular Sciences

ISSN 2075-1303

Global Science Press

Comparison of Gaussian and square laser pulses on molecular orientation

Jingsong Liu[a], Qiyuan Cheng[a], Daguang Yue[a], Xucong Zhou[a] and Qingtian Meng[a]*

Received Nov, 9, 2017,
Accepted Dec. 29, 2017,

DOI: 10.4208/jams.110917.122917a

http://www.global-sci.org/jams/

Abstract. To investigate the orientations of CO molecule driven by both Gaussian and square laser pulses, we give the theoretical analysis using the density matrix method and rigid rotor approximation. The results show that both pulses with a short duration can induce the in-pulse and post-pulse orientations easily, and that the field-free molecular orientation in both non-adiabatic and adiabatic regimes can be obtained by square laser pulse. In addition, the discussion of the temperature effect for field-free orientation shows that the square laser pulse is more feasible in an ensemble of higher temperature.

1. Introduction

These years the laser-induced molecular orientation and alignment techniques have attracted much attention due to their extensive applications in theoretical and experimental researches, such as chemical reaction dynamics [1,2], multiphoton ionization [3,4], high-order harmonic generation [5,6], and photoelectron angular distribution [7,8]. Alignment refers to the molecular axis along laboratory-fixed axes, while the orientation implies that the molecular axis has a specific "head-versus-tail" order. Based on the ratio of the laser pulse duration and the molecular rotational period, there are two alternative ways to obtain the molecular alignment and orientation, i.e., the adiabatic and nonadiabatic regimes. For adiabatic regime, the laser pulse duration is much longer than the molecular rotational period, and the molecular orientation and alignment exists only in the time range of laser excitation [9]. While for nonadiabatic regime, it refers to a reverse case where the laser pulse duration is much shorter than the molecular rotational period and the molecular orientation and alignment can be revived at the rotational period of the molecule after the pulse, which is also called the field-free molecular orientation and alignment [10].

Compared with the molecular alignment, the molecular orientation is more challenging to realize, but has more important applications in related areas. So far, numerous different techniques have been utilized to achieve the molecular orientation. Originally, strong dc-field was used to achieve molecular orientation, however, the orientation degree obtained by this way is relatively low, and strong dc-field may induces the stark effects [11,12]. In later studies, some non-resonant laser fields, such as a two-color laser field and a multi-color laser field were utilized to steer molecular orientation via their interaction with molecular hyperpolarizability [13-15]. However, because of the weak interaction between the laser and the molecular hyperpolarizability, improving the orientation degree needs high intensity of laser pulses, which may lead to the molecular ionization and dissociation. These years with the development of THz technology, some THz laser fields have been used for the realization of field-free molecular orientation, and the often used techniques include the half-cycle THz laser pulse, single-cycle THz laser pulse, and few-cycle THz pulse, which have achieved good results of field-free molecular orientation [16-19]. Recently, many kinds of shaped laser pulse, pulse train and different combined fields were widely used for molecular orientation, and the orientation degree was further improved. Some related works can be referred from the literatures [20-23].

In this paper, we study the molecular orientation of CO induced by Gaussian laser pulse and compare it with one induced by the square laser pulse. In Section 2, the theoretical method of molecular orientation is described in detail. In Section 3, we will firstly study the molecular orientation driven by Gaussian laser pulse and its populations of the rotational states. Then, we compare it with that driven by the square laser pulse and analyse the corresponding populations of the rotational states. In addition, the temperature influence on molecular orientation is also discussed. Finally in Section 4, the conclusions are summarized.

2. Theoretical method

In our scheme, the laser induced molecular orientation is studied for different pulse envelope. The laser field is defined as

$$E(t) = E_1(t)[\cos\omega t + \cos(2\omega t)], \quad (1)$$

$$E_1(t) = E_0 f(t), \quad (2)$$

where E_0 is the amplitude of laser pulse, $f(t)$ is the pulse envelope and ω is the laser frequency. The two different pulse envelopes, viz., Gaussian and square envelope, are, respectively, defined as [24,25]

$$f(t) = \exp(-t^2/2\tau^2), \quad (3)$$

$$f(t) = \begin{cases} 1 & |t| < \tau/2, \\ 0 & \text{others}, \end{cases} \quad (4)$$

where τ is the full width at half maximum. Within the rigid rotor approximation, the total Hamiltonian of the molecule interacting with the laser pulse is given by [26]

$$\hat{H}(t) = B_e\hat{J}^2 - \mu E_1(t)\cos\theta - \frac{1}{4}[(\alpha_{//} - \alpha_\perp)\cos^2\theta + \alpha_\perp]E_1^2(t),$$

$$-\frac{1}{8}[(\beta_{//} - 3\beta_\perp)\cos^3\theta + 3\beta_\perp\cos\theta]E_1^3(t), \quad (5)$$

where the first term is molecular rotational energy with B_e the molecular rotational constant and $\hat{J}$ the angular momentum operator. The second term is the dipole interaction between the laser pulse and the molecule, where μ is the permanent dipole moment. The third and fourth terms are the interactions of laser

School of Physics and Electronics, Shandong Normal University, Jinan, 250014, China
**Corresponding author. E-mail address: qtmeng@sdnu.edu.cn*

pulse with the polarizability and hyperpolarizability, respectively. θ is the angle between the molecular axis and the polarization direction of the laser. $\alpha_{//}(\beta_{//})$ and $\alpha_{\perp}(\beta_{\perp})$ are the polarizabilities (hyperpolarizabilities) parallel and perpendicular to the molecular axis. The degree of molecular orientation is calculated by

$$\langle \cos\theta \rangle = \mathrm{Tr}\{\cos\theta \hat{\rho}(t)\}, \quad (6)$$

where Tr denotes the trace of a matrix and $\hat{\rho}(t)$ is the time-dependent density operator. The time evolution of the density operator can be obtained by solving the quantum Liouville equation,

$$\frac{d\hat{\rho}(t)}{dt} = -\frac{i}{\hbar}[\hat{H}, \hat{\rho}(t)], \quad (7)$$

and the density operator can be expanded in the eigenstates of the rigid rotor Hamiltonian as

$$\hat{\rho}(t) = \sum_{J,M,J',M'} \rho_{JMJ'M'}(t) \left| JM \right\rangle \left\langle J'M' \right|, \quad (8)$$

where $\rho_{JMJ'M'}(t)$ are determined by coupling differential equations [27]

$$\begin{aligned} \frac{\mathrm{d}\rho_{JMJ'M'}(t)}{\mathrm{d}t} &= -\frac{i}{\hbar}\{(\varepsilon_J - \varepsilon_{J'})\rho_{JMJ'M'}(t) \\ &-\mu \mathrm{E}(t)\sum_{J_1M_1}[\rho_{J_1M_1J'M'}(t)V^{(1)}_{JMJ_1M_1} - \rho_{JMJ_1M_1}(t)V^{(1)}_{J_1M_1J'M'}] \\ &-\frac{1}{4}\mathrm{E}^2(t)\Delta\alpha\sum_{J_1M_1}[\rho_{J_1M_1J'M'}(t)V^{(2)}_{JMJ_1M_1} - \rho_{JMJ_1M_1}(t)V^{(2)}_{J_1M_1J'M'}] \\ &-\frac{1}{8}\mathrm{E}^3(t)\sum_{J_1M_1}[(\beta_{//}-3\beta_{\perp})(\rho_{J_1M_1J'M'}(t)V^{(3)}_{JMJ_1M_1} - \rho_{JMJ_1M_1}(t)V^{(3)}_{J_1M_1J'M'}) \\ &+3\beta_{\perp}(\rho_{J_1M_1J'M'}(t)V^{(1)}_{JMJ_1M_1} - \rho_{JMJ_1M_1}(t)V^{(1)}_{J_1M_1J'M'})]\} \end{aligned} \quad (9)$$

where

$$V^{(i)}_{JMJ'M'} = \left\langle JM \left| \cos^i\theta \right| J'M' \right\rangle \ (i = 1,2,3),$$

Above equation can be solved by using the fourth-order Runge-Kutta method. The initial density operator satisfies the temperature-dependent Boltzmann distribution:

$$\rho_0(T) = \frac{1}{Z}\sum_{J=0}^{\infty}\sum_{M=-J}^{M=J}\left| JM \right\rangle \left\langle JM \right| e^{-B_e J(J+1)/K_B T}, \quad (10)$$

where

$$Z = \sum_{J=0}^{\infty}\sum_{M=-J}^{M=J} e^{-B_e J(J+1)/K_B T}, \quad (11)$$

is the partition function with the Boltzmann constant K_B at temperature T.

3. Results and discussion

In this calculation, we take CO as example to study the molecular orientation under the Gaussian and the square pulses. The molecular parameters are set as B_e=1.93cm^{-1}. μ=0.112D, $\alpha_{//} = 2.294\ Å^3$, $\alpha_{\perp} = 1.77\ Å^3$, $\beta_{//} = 2.748\times10^9\ Å^5$, $\beta_{\perp} = 4.994\times10^8\ Å^5$ and the rotational period T_{rot}=8.64ps [28,29]. We first show the time evolution of the molecular orientation induced by Gaussian laser pulse of different pulse duration in Figure 3.1. It can be seen from Figure 3.1(a) that an efficient field-free molecular orientation can be achieved, and the molecular orientation repeatedly revives at around $t = nT_{rot}$ (n=0,1,2…), while Figure 3.1(c) represents a purely adiabatic regime, in which the maximum orientation degree is reached during the laser pulse, and after the laser pulse the orientation vanishes. In Figure 3.1(b) an intermediate case is depicted, where it displays like in the purely adiabatic case during the laser pulse, but the weak field-free orientation remains like the nonadiabatic case after the laser pulse.

To further illustrate the interaction between Gaussian laser pulse and molecules, we show the time evolution of the corresponding rotational population in Figure 3.2. Obviously, before excitation all molecules populate on J=0, then under the stimulation of the fields, the rotational population displays a Rabi-type changing, and after the pulse the population does not change with the time. The periodic field-free molecular orientation shown in Figure 3.1(a) and (b) can be interpreted by that a coherent rotational wave packet is produced after the interaction between the field and molecules, which suffers a periodic dephasing and rephasing when evolving freely in time, i.e., the collapsed wave packet is periodically reconstructed at multiple revival times [30]. For Figure 3.2(c) due to that the pulse duration is enough long, it leads to molecules return to the initial J=0 state after the pulse, and there will be no interference effects, so the field-free orientation cannot be obtained.

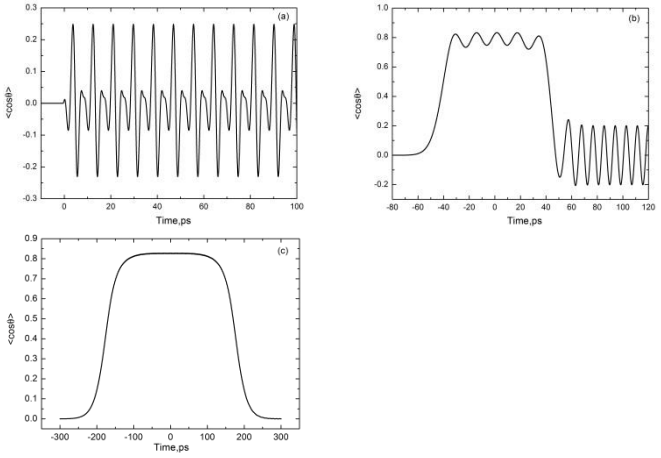

Figure 3.1: The time evolution of the molecular orientation induced by Gaussian laser pulse at $\tau = 0.6$ps (a), $\tau = 50$ps (b) and $\tau = 200$ps (c), where the $E_0 = 6.0\times10^7 Vcm^{-1}$ and T=0K.

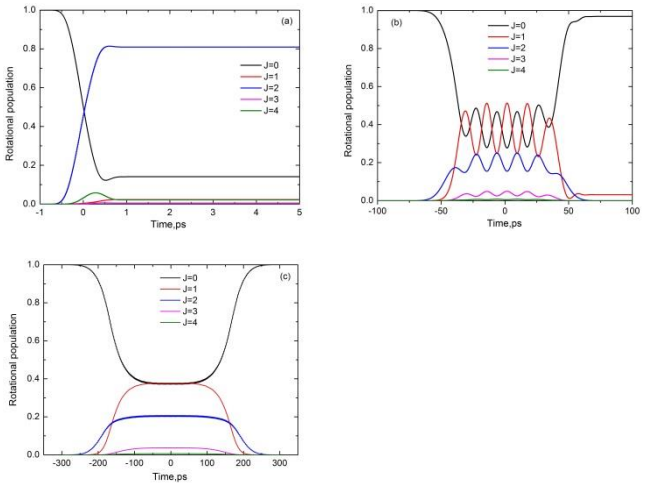

Figure 3.2: The time evolution of the corresponding rotational population induced by Gaussian laser pulse at $\tau = 0.6$ps (a) $\tau = 50$ps (b) and $\tau = 200$ps (c). where the $E_0 = 6.0\times10^7 Vcm^{-1}$ and T=0K.

To see the impact of square laser pulse on molecular orientation, we show the time evolution of the molecular orientation induced by square laser pulse with different pulse duration in Figure 3.3. We find that when $\tau = 0.6\,\mathrm{ps}$, the field-free molecular orientation can be obtained and the maximal orientation degree is a little larger than driven by Gaussian pulse. And when $\tau = 50\,\mathrm{ps}$,both in-pulse and post-pulse orientations are achieved, which is similar to that created by the Gaussian laser pulse. While for $\tau = 200\,\mathrm{ps}$, the field-free molecular orientation can also be realized, which is different from that driven by Gaussian laser pulse. This result indicates that the pulse shape can change the time evolution of the rotational wave packet after the laser pulse, so it has a larger effect on molecular orientation. Furthermore, it can be found that the revival structure of the molecular orientation driven by square laser pulse becomes more complicated than driven by Gaussian laser pulse.

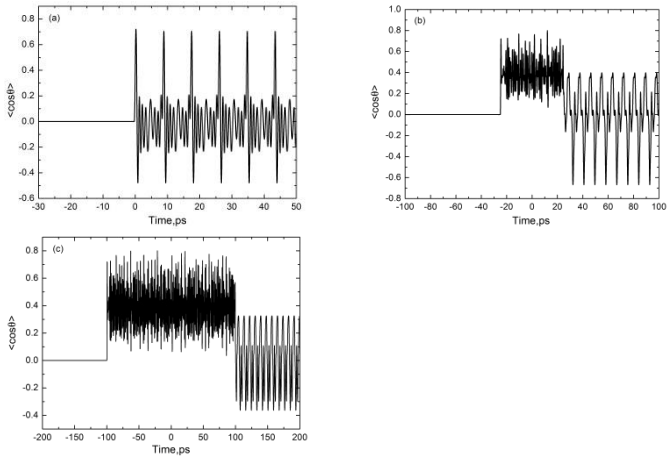

Figure 3.3: The time evolution of the molecular orientation induced by square laser pulse at $\tau = 0.6\mathrm{ps}$ (a) , $\tau = 50\mathrm{ps}$ (b) and $\tau = 200\mathrm{ps}$ (c), where the $E_0 = 6.0 \times 10^7 Vcm^{-1}$ and *T*=0K.

In order to illustrate the physical origin of the above result, we further give the corresponding rotational population induced by square laser pulse in Figure 3.4. It can be found that, comparing with driven by Gaussian laser pulse, the rotational states during square pulse suffer a more intense Rabi-type changing, and the number of the occupied rotational states increases no matter during or after pulse. So the complicated revival structure of the molecular orientation can be explained by the interference contributions of each rotational state. Furthermore, it can be seen from Figure 3.4(c) that for the square laser pulse due to its rapidly vanished field intensity, although the pulse duration is longer, molecules cannot return to the initial *J*=0 state. Instead many rotational states have been populated and formed a coherent rotational wave packet, which evolves freely in time, leading to the filed-free orientation. This appearance is different from that induced by the Gaussian laser pulse.

It is necessary to point out that above calculations are performed at temperature *T* = 0 K. But in actual experiments, the molecular ensemble is at a finite temperature. Here, we give the maximal orientation degree $\langle \cos\theta \rangle_{max}$ as a function of the temperature induced by Gaussian laser pulse (black line) and square laser pulse (red line), respectively in Figure 3.5. Since the thermal movement of molecules can strengthen the disorder of the system, it is natural that the increase of the temperature can lead to the decrease of the degree of maximal molecular orientation. However, when induced by Gaussian laser pulse, the $\langle \cos\theta \rangle_{max}$ decreases rapidly with the increase of temperature, while for driven by square laser pulse, the $\langle \cos\theta \rangle_{max}$ decreases slowly. This is because the square laser pulse has a flatter top and rapidly intensity decline which leads to a longer duration of its maximum intensity, so it is easier to overcome the impact of thermal movement. Consequently, the square laser pulse is more feasible in an ensemble of higher temperature.

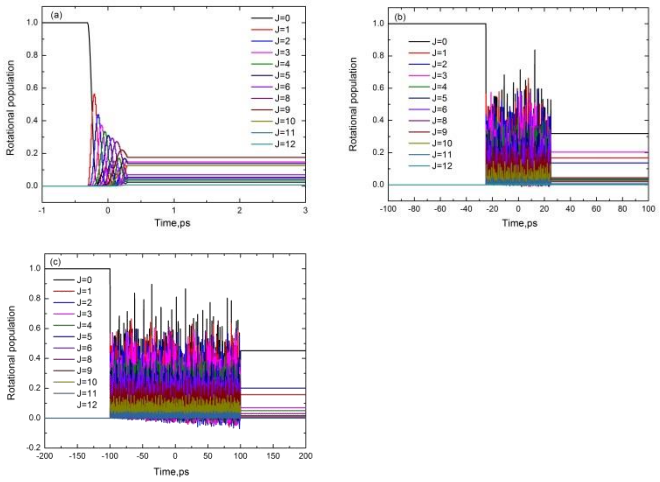

Figure 3.4: The time evolution of the corresponding rotational population induced by square laser pulse at $\tau = 0.6\mathrm{ps}$ (a) $\tau = 50\mathrm{ps}$ (b) and $\tau = 200\mathrm{ps}$ (c). where the $E_0 = 6.0 \times 10^7 Vcm^{-1}$and *T*=0K.

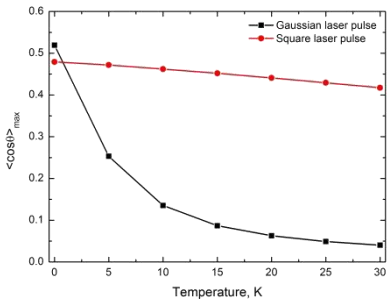

Figure 3.5: The maximal orientation degree $\langle \cos\theta \rangle_{max}$ as a function of the temperature induced by Gaussian laser pulse (black line) and square laser pulse (red line), respectively, where the $E_0 = 9.0 \times 10^7 Vcm^{-1}$ and $\tau = 0.6\mathrm{ps}$.

4. Conclusions

In summary, we have theoretically studied the molecular orientation driven by Gaussian laser pulse and compared it with driven by the square laser pulse. It is shown that when the durations of both Gaussian and square laser pulse are short, the in-pulse and post-pulse orientations can be induced. Compared with driven by Gaussian laser pulse, the field-free molecular orientation induced by the square laser pulse can be achieved in both non-adiabatic and adiabatic regimes. Increasing temperature has an inhibitory effect on molecular orientation for both laser pulses, but

the square laser pulse is more feasible in an ensemble of higher temperature.

Acknowledgements

This work was supported by National Natural Science Foundation of China (Grant No. 11674198), Taishan scholar project of Shandong Province, and Shandong Province Natural Science Foundation (Grant No. ZR2014AM002).

References

[1] S. Fleischer, I. Sh. Averbukh, Y. Prior, Phys. Rev. A, 74 (2006) 041403
[2] H. Stapelfeldt and T. Seideman, Rev. Mod. Phys., 75 (2003) 543
[3] T. Suzuki, S. Minemoto, T. Kanai and H. Sakai, Phys. Rev. Lett., 92(2004) 133005
[4] I. V. Litvinyuk, K. F. Lee, P. W. Dooley, D. M. Rayner, D. M. Villeneuve, P. B. Corkum, Phys. Rev. Lett., 90 (2003) 233001
[5] T. Kanai, S. Minemoto, H. Sakai, Nature, 435 (2005), 470
[6] T. Kanai, S. Minemoto, H. Sakai, Phys. Rev. Lett., 98 (2007) 053002
[7] J. Itatani, J. Levesque, D. Zeidler, H. Niikura, H. P´epin, J. C. Kieffer, P. B. Corkum, D. M. Villeneuve, Nature, 432 (2004) 867
[8] J. L. Hansen, H. Stapelfeldt, D. Dimitrovski, M. Abu-Samha, C. P. Martiny and L. B. Madsen, Phys. Rev. Lett., 106 (2011) 073001
[9] H. Sakai, C. P. Safvan, J. J. Larsen, K. M. Hilligsøe, K. Hald, H. Stapelfeldt, J. Chem. Phys., 110 (1999) 10235
[10] A. Goban, S. Minemoto and H. Sakai, Phys. Rev. Lett., 101 (2008) 013001
[11] B. Friedrich and D. R. Herschbach, Z. Phys. D, 18 (1991) 153
[12] H. Sakai, S. Minemoto, H. Nanjo, H. Tanji and T. Suzuki, Phys. Rev. Lett., 90 (2003) 083001
[13] J. Wu and H. P. Zeng, Phys, Rev. A, 81 (2010) 053401
[14] S. A. Zhang, C. H. Lu, T. Q. Jia, Z. G. Wang and Z. R. Sun, J. Chem. Phys., 135 (2011) 034301
[15] S. W. Xu, Y. H. Yao, C. H. Lu, T. Q. Jia, J. X. Ding, S. A. Zhang and Z. R. Sun, Phys. Rev. A, 90 (2014) 033416
[16] A. Matos-Abiague and J. Berakdar, Phys. Rev. A, 68 (2003) 063411
[17] C. C. Shu, K. J. Yuan, W. H. Hu and S. L. Cong, J. Chem. Phys., 132 (2010) 244311.
[18] Z. Y. Zhao, Y. C. Han, Y. Huang and S. L. Cong, J. Chem. Phys., 139 (2013) 044305
[19] C. C. Qin, Y. Tang, Y. M. Wang and B. Zhang, Phys. Rev. A, 85 (2012) 053415
[20] M. Muramatsu, M. Hita, S. Minemoto and H. Sakai, Phys. Rev. A, 79 (2009) 011403
[21] J. Salomom, C. M. Dion, G. Turinici, J. Chem. Phys., 123 (2005) 144310
[22] H. P. Dang, S. Wang, W. S. Zhan, J. B. Zai and X. Han, Chem. Phys., 461 (2015) 81
[23] H. Li, W. X. Li, Y. H. Feng, H. F. Pan, H. P. Zeng, Phys. Rev. A, 88 (2013) 013424
[24] Y. Liu , J. Li, J. Yu and S. L. Cong, Laser. Phys. Lett., 10 (2013) 076001
[25] U. Arya and V. Prasad, Phys. Rev. A, 87 (2013) 035402
[26] S. A. Zhang, J. H. Shi, H. Zhang, T. Q. Jia, Z. G.Wang, Z. R. Sun, Phys. Rev. A, 83 (2011) 023416
[27] S. Ramakrishna and T. Seideman, J. Chem. Phys., 124 (2006) 034101
[28] K. A. Peterson, T. H. Dunning, J. Mol. Struc-Theochem, 400 (1997) 93
[29] M. Pecul, Chem. Phys. Lett., 404 (2005) 217
[30] R. Torres, R. de Nalda, J. P. Marangos, Phys. Rev. A, 72 (2005) 023420